NASA TECHNICAL MEMORANDUM

NASA TM X-71487

NASA TM X-71487

PERFORMANCE OF EPITAXIAL BACK SURFACE FIELD CELLS

by Henry W. Brandhorst, Jr., Cosmo R. Baraona, and Clifford K. Swartz
Lewis Research Center
Cleveland, Ohio 44135

TECHNICAL PAPER proposed for presentation at Tenth Photovoltaic Specialists Conference sponsored by the Institute of Electrical and Electronics Engineers Palo Alto, California, November 13-15, 1973

PERFORMANCE OF EPITAXIAL BACK SURFACE FIELD CELLS

by Henry W. Brandhorst, Jr., Cosmo R. Baraona, and Clifford K. Swartz

National Aeronautics and Space Administration
Lewis Research Center
Cleveland, Ohio

SUMMARY

Epitaxial back surface field structures were formed by depositing a 10 μm thick 10 Ω-cm epitaxial silicon layer onto substrates with resistivities of 0.01, 0.1, 1.0 and 10 Ω-cm. A correlation between cell open-circuit voltage and substrate resistivity was observed and was compared to theory. The cells were also irradiated with 1 MeV electrons to a fluence of 5×10^{15} e/cm^2. The decrease of cell open-circuit voltage was in excellent agreement with theoretical predictions and the measured short circuit currents were within 2% of the prediction. Calculations are presented of optimum cell performance as functions of epitaxial layer thickness, radiation fluence and substrate diffusion length.

E-7820

INTRODUCTION

Back surface field effect (BSF) solar cells made from 10 Ω-cm material exhibit open-circuit voltages and efficiencies higher than conventional 10 Ω-cm cells (1-3). The increased voltage appears to be dependent upon the ratio of base width, W, to base minority carrier diffusion length, L. (1,4) Small ratios lead to higher voltages and hence increased performance over conventional 10 Ω-cm cells. In order to retain this performance advantage in a radiation field, which decreases L, it is necessary that the W/L ratio in the BSF cell remain small. Published results (1) indicate that 100 μm thick BSF cells retain their open circuit voltage advantage over conventional cells to higher electron fluences than do thicker BSF cells. Fabrication of single crystal cells with base widths less than 100 μm poses a handling problem. Therefore, Mandelkorn (1) proposed the epitaxial structure shown in figure 1 to circumvent these handling problems. This structure differs from the epitaxial drift field solar cell structures fabricated in the past (5-7) in that there is no intentional gradation of dopant throughout the epitaxial layer.

The purpose of this work was to confirm feasibility of the epitaxial BSF concept and to explore the performance of epitaxial BSF solar cell structures having base widths of about 10 μm. This layer thickness was chosen primarily to test theoretical predictions of open-circuit voltage and degradation in a radiation field rather than to optimize output. The layers were deposited onto substrates with resistivities between 10 and 0.1 Ω-cm. Solar cells were formed, tested, then irradiated with 1 MeV electrons to fluences of 5×10^{15} e/cm^2. The performance of these cells was compared to theoretical predictions. Optimization of the epitaxial BSF structure as a function of radiation fluence was also calculated.

THEORY

The simple diode equation of Shockley (8) was used to model the open-circuit voltage, V_{oc}, through the following relationship:

$$V_{oc} = \frac{kT}{q} \ln \frac{I_L}{I_o} \tag{1}$$

where I_L is the light generated current and I_o the reverse saturation current. The terms k, T, and q have their usual meanings. I_o was modelled using the low-high junction theory of Godlewski et al. (4). The following relationship was obtained for I_o

$$I_{o_p} = \frac{qn_i^2 D_p}{N_A L_p} \left\{ \frac{S + \tanh \frac{W_p}{L_p}}{1 + S \tanh \frac{W_p}{L_p}} \right\} \tag{2}$$

where

$$S = \frac{N_A}{N_{A^+}} \frac{D_{p^+}}{D_p} \frac{L_p}{L_{p^+}} \left\{ \frac{\frac{s_r L_{p^+}}{D_{p^+}} + \tanh \frac{W_{p^+}}{L_{p^+}}}{1 + \frac{s_r L_{p^+}}{D_{p^+}} \tanh \frac{W_{p^+}}{L_{p^+}}} \right\}, \tag{2a}$$

where W_p is the p-type region width, L_p and L_{p^+} are electron diffusion lengths and D_p and D_{p^+} are electron diffusion constants in the p and p$^+$ regions. W_{p^+} is p$^+$ region thickness and s_r is the surface recombination velocity at the metal-p$^+$ region contact. The other terms are in standard notation. The total I_o must also include the I_{o_n} component from the diffused region. The drift field model was used for this component as described previously (4). However, because its magnitude was much lower than I_{o_p}, I_{o_n} was ignored for the calculations.

Equation (2) was used to model 10 Ω-cm epitaxial structures deposited on 1, 0.1, or 0.01 Ω-cm substrates. This construction produces back surface field structures due to autodoping of the epitaxial layer by the substrate. For the structures formed on 10 Ω-cm substrates, the finite width, infinite surface recombination velocity model for I_o was used because no back surface field was formed there. The I_{o_∞} relationship for this case is:

$$I_{o_\infty} = qn_i^2 \left[\frac{D_n}{N_A L_n} \coth \frac{W_n}{L_n} + \frac{D_p}{N_D L_p} \coth \frac{W_p}{L_p} \right] \tag{3}$$

where the terms have their usual meanings.

Performance in a radiation environment was determined by using equations (1-3). The radiation-reduced diffusion length at each fluence level was obtained using the standard relationship:

$$\frac{1}{L_\Phi^2} = \frac{1}{L_O^2} + K\Phi \tag{4}$$

where L_Φ is the diffusion length at a given fluence, L_O the initial diffusion length, Φ the fluence of 1 MeV electrons and K the damage coefficient. The damage coefficient used for the epitaxial layer was 9×10^{-11}/electron (9).

EXPERIMENTAL

Cell Fabrication

A cross section of the epitaxial cell structure is shown in figure 1. Substrates used in the epitaxial deposition were 10, 1, 0.1, and 0.01 Ω-cm resistivity with dimensions 1×2×0.035 cm. Prior to epitaxial deposition, the wafers were mechanically polished. They were then placed in an epitaxial reactor with the lowest resistivity samples at the downstream end of the gas inlet. The deposition sequence consisted of a 6 min. heat-up in hydrogen to the deposition temperature of 1125° C followed by a 4 min. etch in HCl. After purging with H_2, a $SiCl_4$-B_2H_6-H_2 mixture was passed through the chamber for about 14 minutes to form the epitaxial Si layer. After a 1/2 minute purge with H_2 the samples were removed. In one of the depositions, a 9.0 μm epitaxial layer of 9.8 Ω-cm average resistivity was obtained. In the other deposition a malfunction occurred after a 6.0 μm thick layer of 5.8 Ω-cm material had been deposited. Subsequently, a 2.6 μm layer of 15 Ω-cm material was deposited to complete the run. Junctions were then formed in the wafers by diffusion from a $POCl_3$ source at 850° C for 30 min. Contacts were applied to complete fabrication. No antireflection coatings were used on the cells.

Performance Evaluation

Performance evaluation of the cells was made under a Spectrolab X-25L solar simulator. Spectral responses were obtained with narrow bandpass interference filters (10). Diffusion length measurements were made using the x-ray technique (11). Ionized impurity profiles in the epitaxial layers were obtained from capacitance-voltage measurements.

Irradiations were performed in air using 1 MeV electrons from a Cockroft-Walton type accelerator (10). Samples were mounted on a temperature controlled plate. Cell performance was monitored periodically during irradiation. Maximum irradiation fluence was 5×10^{15} e/cm^2.

EXPERIMENTAL RESULTS

Performance Prior to Irradiation

Efficiency. - Of the 60 substrates coated with epitaxial silicon layers, 36 were fabricated into solar cells. Nine cells were made from each of the four substrate resistivities -- 0.01, 0.1, 1.0 and 10 Ω-cm. Junction characteristics were good and reverse leakage currents were low. Some cells had high series resistances that were traced to grids that did not adhere well to the polished surfaces. This was a slight problem; however about half of the cells had fill factors in excess of 72% initially. The maximum fill factor initially was nearly 76%.

The dependence of cell efficiency on substrate resistivity is shown in figure 2. The points represent the average of nine cells, and the bars the range. Cells made on the 1.0 Ω-cm substrates had the highest efficiency. Average cell efficiency was 6.2%, which corresponds to 8.4% if an antireflection coating such as SiO had been applied.

Short Circuit Current. - The dependence of short-circuit current on substrate resistivity is shown in figure 3. Again, the range is indicated by the bars and the points represent the average of 9 cells. If only the 10μm epitaxial layer were contributing to the short-circuit current, a current of about 41 mA would be expected. This is true for only the 0.01 Ω-cm substrate cells. Significant contributions to cell current are apparently being made by the substrates in the other cases.

The peak in cell current for the 1.0 Ω-cm cells was unexpected and caused the peak in cell efficiency noted previously. Measurements of diffusion lengths made on companion wafers prior to deposition indicated that the short-circuit currents should have increased continuously from 0.01 to 10 Ω-cm substrates. This trend holds for all except the 10 Ω-cm substrates where the decrease is noted. To test if a loss of diffusion length had occurred during the epitaxial deposition, the epitaxial layer was removed and a conventional cell made from the 10 Ω-cm substrate. Subsequent diffusion length and cell performance measurements indicated that the diffusion length had indeed decreased to about 50 μm. No diffusion length measurements were made on the other substrates after processing to determine if similar diffusion length degradation had occurred.

Attempts to determine diffusion lengths in the epitaxial cells were frustrated by the difficulty of interpreting the results. In addition to significant current contributions from the substrate, the presence of a back surface field further complicated the results.

Open Circuit Voltage. - The dependence of open-circuit voltage, V_{oc}, on substrate resistivity is shown in figure 4. The bars represent the range of experimental results obtained. The solid curve was obtained from equations (1), (2) and (2a) using the data shown in Table I for the cells on 0.01, 0.1 and 1.0 Ω-cm substrates. Conventional theory was used for the cells on 10 Ω-cm substrates. Current densities were obtained from figure 3. The values of substrate diffusion lengths were obtained from measurements described previously. The constant value of diffusion length in the epitaxial layer of 80 μm was chosen to provide a good fit to the data at the 0.01 Ω-cm point. Good agreement is obtained for all resistivities. No increase in V_{oc} is predicted for substrate resistivities below 0.1 Ω-cm in agreement with data from Mandelkorn (12).

Closer inspection of the experimental data shows that variations from cell to cell cause the wide range of values indicated. For example, the average open-circuit voltages of cells formed in a single deposition run are consistently greater than the voltages of cells formed when two depositions were required. From the deposition data, it was known that the doping profiles were different between the two cases. To obtain more quantitative information, capacitance-voltage measurements were made to determine the impurity profile in the first several microns of the epitaxial layer nearest the junction. Results for typical single and double deposition cells are shown in figure 5. It can clearly be seen that the deposition did not result in uniformly doped layers. Although the average resistivity of the layer formed in a single deposition was measured to be 9.8 Ω-cm, it can be seen from figure 5 that the material closest to the junction was about 6 Ω-cm. In the double deposition case, 15 Ω-cm material is closest to the junction. The 6 and 15 Ω-cm resistivities were then used instead of the average of 10 Ω-cm to model the cells deposited on 10 Ω-cm substrates. The complete range of open-circuit voltages observed in figure 4 for the 10 Ω-cm substrates was predicted.

Since reverse breakdown limits C-V measurements, it was not possible to measure profiles deeper into the wafer without etching away some material. No etching was done, hence the autodoping profile of the p^+ substrate into the epitaxial layer was not determined. It should also be noted that a slightly harmful drift

field is present in the single deposition cells, while a slightly beneficial drift field is present in the double deposition cells. These slight profile differences apparently did not greatly affect the results.

Performance After Irradiation

Open Circuit Voltage. - Figure 6 shows the effect of 1 MeV electron irradiation on the open-circuit voltage of epitaxial cells formed on the different substrates. The points for each substrate resistivity are the average of three cells. Also included are results for conventional 10 Ω-cm cells (13). Epitaxial cells formed on 0.01, 0.1 or 1 Ω-cm substrates have greater open-circuit voltages than conventional cells at all fluences. The performance of the epitaxial cells formed on 10 Ω-cm substrates is typical of a conventional cell having an initial diffusion length of about 80 μm. This is consistent with the results of figure 3. The epitaxial cells formed on 0.01 Ω-cm substrates had the highest open-circuit voltages and they retained this advantage throughout the irradiation. Therefore the data from these cells were used to test predictions made from theory. These cells were also the easiest to model because their substrate diffusion lengths were low -- probably less than 5 μm. Figure 7 shows the results obtained using equations (1), (2) and (2a) when an initial diffusion length of 80 μm was assumed for the epitaxial layer and 3 μm for the substrate. Temperature was 25° C and a layer thickness of 9.0 μm was assumed. No attempt was made to account for the different impurity concentration near the interface. A diffusion length damage coefficient of 9×10^{-11}/electron was used for the epitaxial layer. No change was made in the 0.01 Ω-cm substrate diffusion length. The error bars show the range of results obtained and the points represent the averages. Excellent agreement is obtained between theory and experiment. The range of values obtained for the cells may be due to the variation in doping level near the junction. Also, the voltage of the point at 5×10^{15} e/cm^2 may be in some error because significant peeling of the grids from the cell occurred at that point.

Short Circuit Current. - Figure 8 shows the variation in short-circuit current with 1 MeV electron fluence for epitaxial cells formed on the different resistivity substrates. Again, the 1.0 Ω-cm substrate cells have the highest currents as noted previously. Typical of all curves is the slight decrease in current as a function of fluence. Above 2×10^{15} e/cm^2 however, there is a substantial decrease in current. This was caused by a catastrophic loss of grid adherence with a concommitant increase in cell series resistance as mentioned before.

Figure 9 shows the results comparing theoretical predictions of short-circuit current degradation for the 0.01 Ω-cm substrate cells. The parameters assumed were the same as for the open circuit voltage case. The data points at 5×10^{15} e/cm^2 were deleted because of the series resistance problem. Low-high junction theory was used to model the current and the derivation of the equations will be described elsewhere (14). The theoretical curve agrees within 2% of the experimental curve. This difference may easily be accounted for by the inability to accurately set the solar simulator. No standard cell whose spectral response matched the test cells was available. To further corroborate this contention, a comparison between cell short-circuit current obtained under the X-25L solar simulator and those obtained using the filter wheel solar simulator (15) indicates that the solar simulator results may be up to 2% low for these 0.01 Ω-cm substrate cells. In any case, good agreement between theory and experiment is obtained.

EPITAXIAL CELL OPTIMIZATION

Because of the excellent agreement between the experimental and theoretical results, calculations were made to optimize the epitaxial back surface field cell structure for performance in a radiation field. These calculations were performed using the low-high junction theory (4, 14) described previously. In this study, efficiency was calculated as a function of epitaxial layer thickness and fluence of 1 MeV electrons. These efficiencies were calculated for cells with an ideal SiO antireflection coating, a 0.01 Ω-cm substrate and an ideal fill factor. As a result of the ideal fill factor assumption, these efficiencies are about 15% greater than could be practically achieved but serve well for relative comparisons. The values used in this calculation are shown in Table II and the results shown in figures 10 and 11. In figure 10, an initial substrate diffusion length of 3 μm with a damage coefficient of 9×10^{-10} electron^{-1} was assumed. The initial epitaxial layer diffusion length was held constant at 100 μm independent of layer thickness. The diffusion length damage coefficient used for the epitaxial layer was 9×10^{-11}/electron.

It can be seen that peak efficiency depends on both the width of the epitaxial layer and the fluence. For each end-of-life fluence, there is an optimum epitaxial layer thickness that gives maximum efficiency at end-of-life. For example, for a fluence of 1×10^{15} electrons/cm^2 corresponding to about 22 years in synchronous orbit, a peak efficiency of 10.8% is obtained with an epitaxial layer thickness of 17 μm. For epitaxial layers thicker than about 200 μm, the effect of the back surface field is not observed and the cell behaves like a conventional cell. Accordingly, conventional cell performance is represented by the calculated values at 300 μm thickness. Using this comparison, it can be seen that at all fluences the optimum thickness epitaxial layer cell will outperform the conventional cell by about 5%.

In the second case, an initial 50 μm diffusion length was assumed in the 0.01 Ω-cm substrate. This substrate diffusion length was assumed to degrade with a damage coefficient of 9×10^{-10}/electron and for the 10 Ω-cm epitaxial layer damage coefficient was the 9×10^{-11}/electron used previously. The effect of having a significant substrate diffusion length is clearly shown in figure 11. In this case, the efficiency is not as strongly dependent on epitaxial layer thickness. As a result, a 6-10 μm epitaxial layer would provide essential peak performance at all fluence levels. In this case, at a fluence level of 1×10^{15} e/cm^2, the peak efficiency for a 10 μm epitaxial layer thickness is 11.1% compared to 10.8% for the previous epitaxial cell calculation and 10.2% for the conventional cell as noted by the 300 μm epitaxial layer thickness case. (Once again the efficiencies are theoretical efficiencies; practical efficiency would be about 15% lower.) Thus the presence of a significant diffusion length in the substrate leads to a much improved device producing nearly 10% more power than the conventional cell.

DISCUSSION

As discussed elsewhere (4), the major unanswered question relating to the low-high junction (LHJ) theory is that of diffusion length. As was shown in this paper, excellent agreement is obtained between LHJ theory and the experimental results provided long diffusion lengths are present in the very thin epitaxial layer. In this work, a diffusion length of 80 μm was needed to fit the initial data. Whether this long a diffusion length existed in this layer is speculative at this time. Attempts to measure this diffusion length

proved futile, as interpretation of the results was complicated by the presence of a substrate with a significant diffusion length as well as the back surface field. Clearly, additional work must be performed to resolve this question. However, the success of the low-high junction theory at explaining the variation of open-circuit voltage with substrate resistivity and the variation of both open-circuit voltage and short-circuit current with electron fluence suggests the validity of this approach.

CONCLUSIONS

As a result of this study, the following conclusions can be made:

1. Back surface field effects can be achieved by epitaxial deposition of 10 Ω-cm silicon layers onto substrates with lower resistivities.

2. The electrical characteristics of these cells are similar to other back surface field cells.

3. Low-high junction theory explains the variation in open-circuit voltage with substrate resistivity, and the variation of both the open-circuit voltage and short-circuit current with radiation fluence, provided an initial diffusion length of about 80 μm in the epitaxial layer is assumed.

4. Optimization of the epitaxial cell structure leads to the conclusion that substrate diffusion length can significantly influence cell performance. If the substrate diffusion length is low, performance in a radiation field is critically dependent upon epitaxial layer thickness. However, if the substrate diffusion length is long, superior performance results and there is only a very weak dependence on epitaxial layer thickness. In the latter case a peak theoretical efficiency of 11.1% at 1×10^{15} e/cm^2 was obtained. This can be compared to a theoretical efficiency of 10.2% for a conventional cell at the same fluence.

REFERENCES

1. J. Mandelkorn and J. H. Lamneck, Jr., "Simplified Fabrication of Back Surface Electric Field Silicon Cells and Novel Characteristics of Such Cells," NASA TM X-68060, May 1972.

2. P. A. Iles, "Increased Output from Silicon Solar Cells," Conference Record of the Eighth IEEE Photovoltaic Specialists Conference, Seattle, WA., Aug. 1970, p. 345.

3. H. Fischer, E. Link and W. Pschunder, "Influence of Controlled Lifetime Doping on Ultimate Technological Performance of Silicon Solar Cells," Conference Record of the Eighth IEEE Photovoltaic Specialists Conference, Seattle, WA., Aug. 1970, p. 70.

4. M. P. Godlewski, C. R. Baraona and H. W. Brandhorst, Jr., "Low-High Junction Theory Applied to Solar Cells," Conference Record of the Tenth IEEE Photovoltaic Specialists Conference, Palo Alto, CA., Nov. 1973.

5. W. R. Runyan and E. G. Alexander, "Development of Epitaxial Structures for Radiation Resistant Solar Cells," Proceedings of the Fifth Photovoltaic Specialists Conference, Greenbelt, MD., Oct. 1965, Vol. I, #A-2.

6. K. S. Tarneja, R. K. Riel, V. A. Rossi and E. R. Stonebraker, "Drift Field Dendritic Solar Cells," Proceedings of the Fifth Photovoltaic Specialists Conference, Greenbelt, MD., Oct. 1965, Vol. I, #A-3.

7. K. Tarneja, J. Hicks, R. Babcock and E. Stonebraker, "Radiation Resistance of Webbed Dendritic Solar Cells," Proceedings of the Fourth Photovoltaic Specialists Conference, Cleveland, OH., June 1964, Vol. I, #A-8.

8. W. Shockley, "The Theory of p-n Junctions in Semiconductors and p-n Junction Transistors," Bell Syst. Tech. J., vol. 28, p. 435, 1949.

9. R. G. Downing, J. R. Carter, Jr. and J. M. Denney, "The Energy Dependence of Electron Damage in Silicon," Proceedings of the Fourth Photovoltaic Specialists Conference, Cleveland, OH., June 1964, Vol. I, #A-5.

10. H. W. Brandhorst, Jr. and R. E. Hart, Jr., "Radiation Damage to Cadmium Sulfide Solar Cells," NASA TN D-2932, July 1965.

11. J. H. Lamneck, Jr., "Diffusion Lengths in Silicon Obtained by an X-ray Method," NASA TM X-1894, Oct. 1969.

12. J. Mandelkorn, J. H. Lamneck, Jr. and L. R. Scudder, "Design, Fabrication and Characteristics of New Types of Back Surface Field Cells," Conference Record of the Tenth IEEE Photovoltaic Specialists Conference, Palo Alto, CA., Nov. 1973.

13. W. R. Cherry and R. L. Statler, "Photovoltaic Properties of U.S. and European Silicon Cells under 1 MeV Electron Irradiation," NASA TM X-63272, Apr. 1968.

14. M. P. Godlewski, C. R. Baraona and H. W. Brandhorst, Jr., "Low-High Junction Theory Applied to Solar Cells - Short Circuit Current Relationships" To be published.

15. J. Mandelkorn, J. D. Broder and R. P. Ulman, "The Filter Wheel Solar Simulator," NASA TN D-2562, Jan. 1965.

TABLE I

PARAMETERS USED IN CALCULATION OF OPEN CIRCUIT VOLTAGE VARIATION WITH SUBSTRATE RESISTIVITY

SUBSTRATE					EPITAXIAL LAYER		
Resistivity Ω-cm	Mobility cm^2/v-sec	Diffusion Length Microns	Width Microns	Resistivity Ω-cm	Mobility cm^2/v-sec	Diffusion Length Microns	Thickness Microns
0.01	125	5	300	10	1275	80	10
0.1	360	50	300	10	1275	80	10
1.0	850	125	300	10	1275	80	10
10	1275	50	300	10 Nominal (15/6 or 6)	1275 1325-1200	80	10

TABLE II

DATA FOR OPTIMIZATION OF EPITAXIAL BSF CELL

Air Mass Zero Spectrum
300 K Temperature
SiO Coated Cell
0.25 μm Junction Depth
Surface Recombination Velocities
- Front - 10^5 cm/sec
- Back - 10^8 cm/sec

Epitaxial Layer Properties
- Initial Diffusion Length - 100 μm
- Damage Coefficient - 9×10^{-11} electron^{-1}

Substrate Properties
- 250 μm Thick, 0.01 Ω-cm Material
- Initial Diffusion Length
  - Fig. 10 - 3 μm
  - Fig. 11 - 50 μm
- Damage Coefficient - 9×10^{-10} electron^{-1}

CROSS SECTION OF EPITAXIAL
BACK SURFACE FIELD CELL

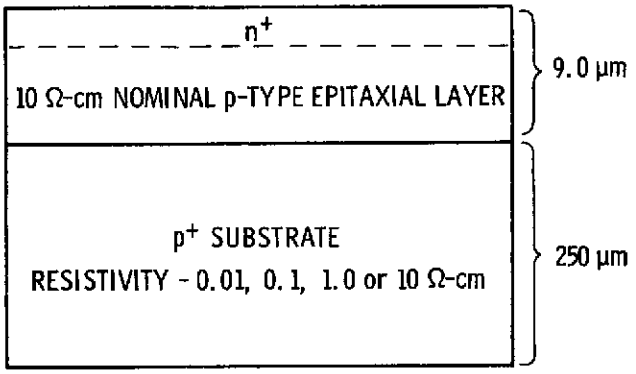

Fig. 1

VARIATION OF EPITAXIAL CELL EFFICIENCY
WITH SUBSTRATE RESISTIVITY

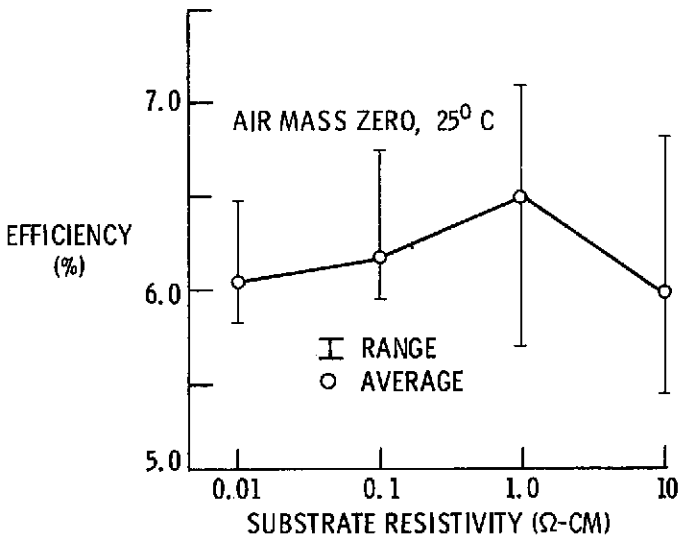

Fig. 2

VARIATION OF EPITAXIAL CELL SHORT-CIRCUIT CURRENT WITH SUBSTRATE RESISTIVITY

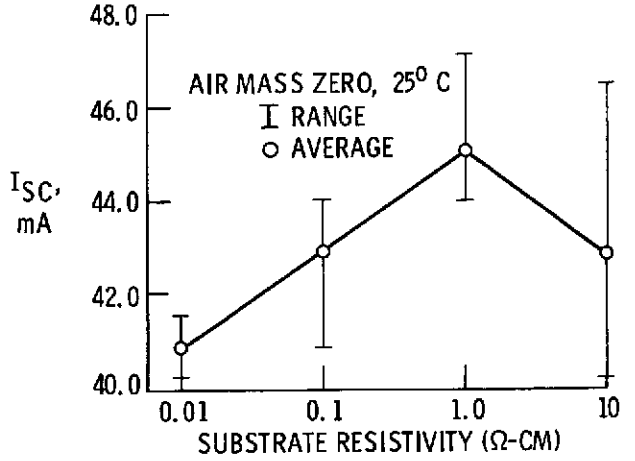

Fig. 3

VARIATION OF EPITAXIAL CELL OPEN CIRCUIT VOLTAGE WITH SUBSTRATE RESISTIVITY

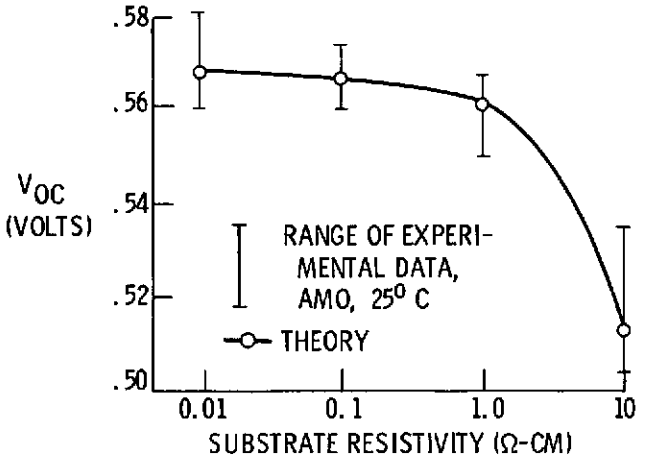

Fig. 4

VARIATION OF IMPURITY PROFILE IN EPITAXIAL LAYERS

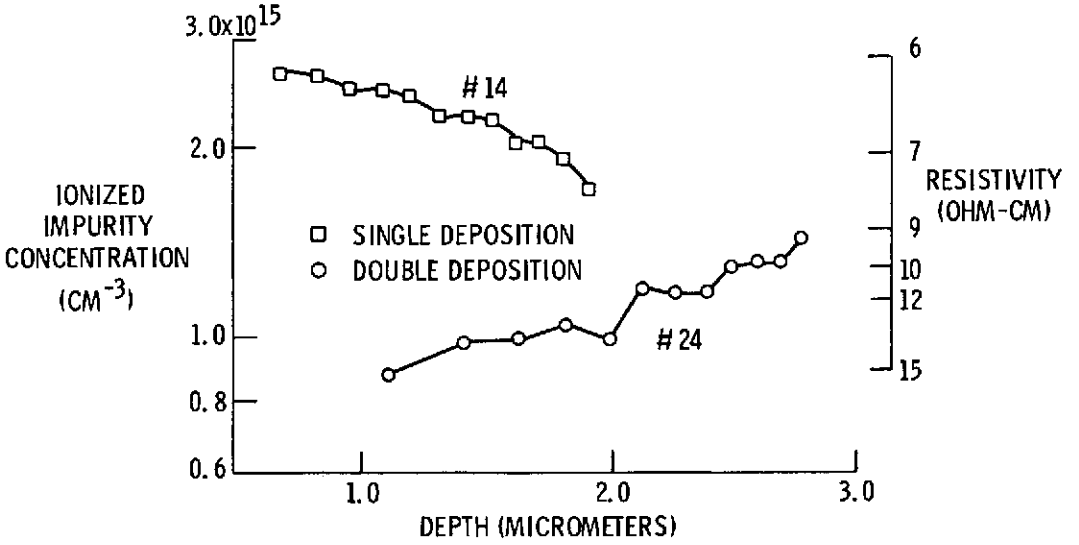

Fig. 5

E-7820

EFFECT OF SUBSTRATE RESISTIVITY ON THE VARIATION OF OPEN CIRCUIT VOLTAGE UNDER ELECTRON IRRADIATION

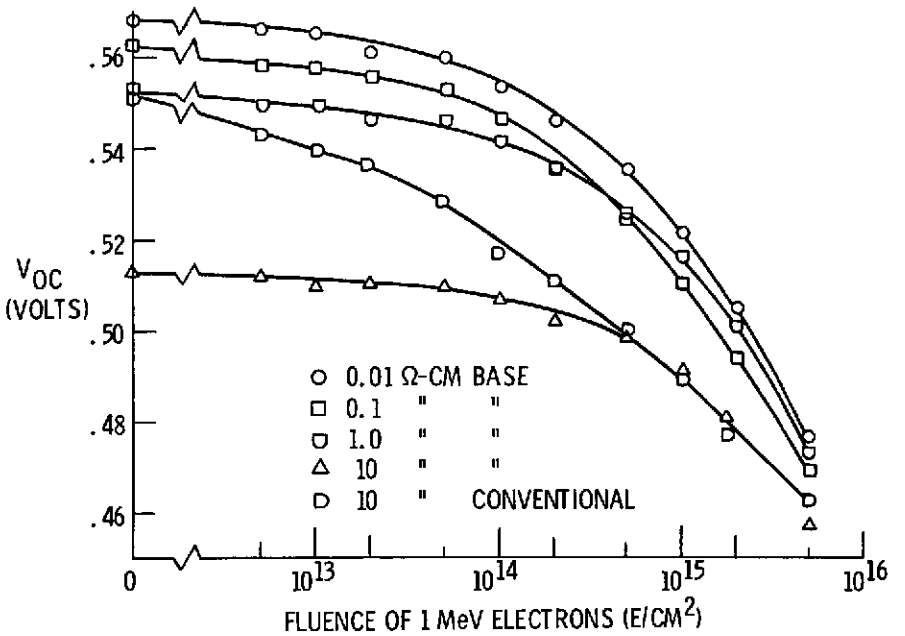

Fig. 6

VARIATION OF OPEN-CIRCUIT VOLTAGE OF 0.01 Ω-CM SUBSTRATE CELLS WITH 1 MeV ELECTRON FLUENCE

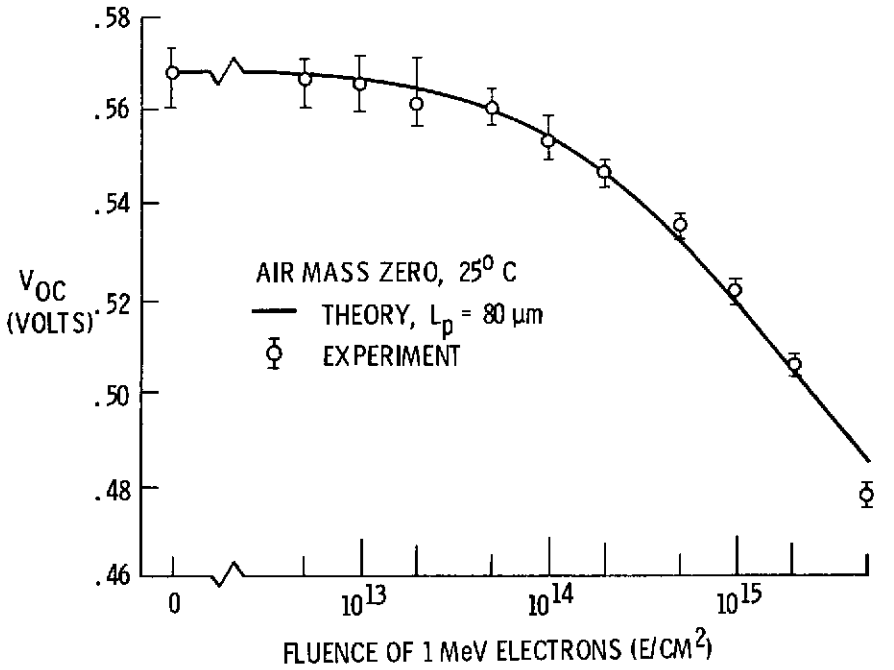

Fig. 7

EFFECT OF SUBSTRATE RESISTIVITY ON THE VARIATION OF SHORT CIRCUIT CURRENT UNDER ELECTRON IRRADIATION

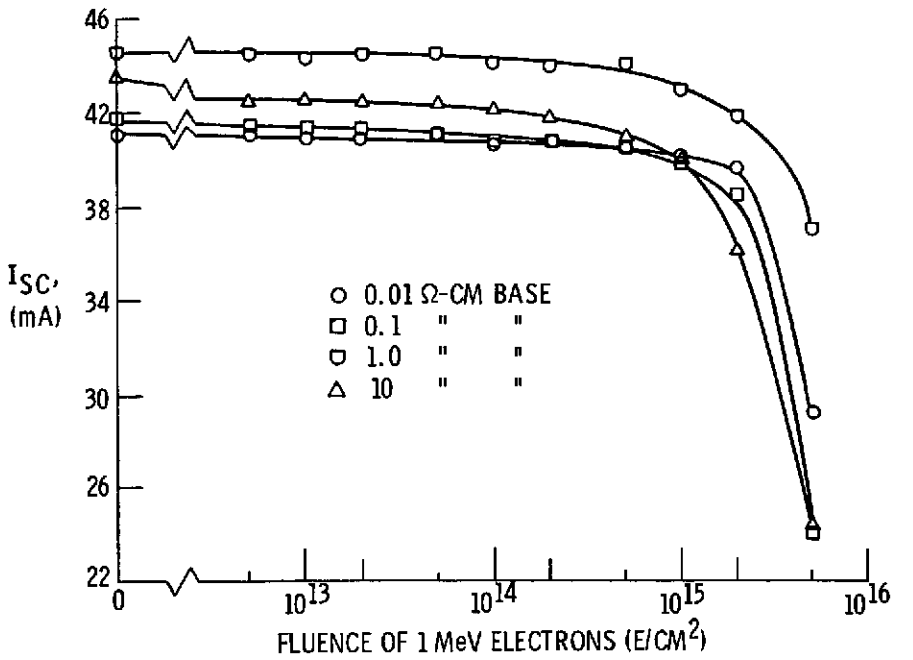

Fig. 8

VARIATION OF SHORT-CIRCUIT CURRENT OF 0.01 Ω-CM SUBSTRATE CELLS WITH ELECTRON IRRADIATION

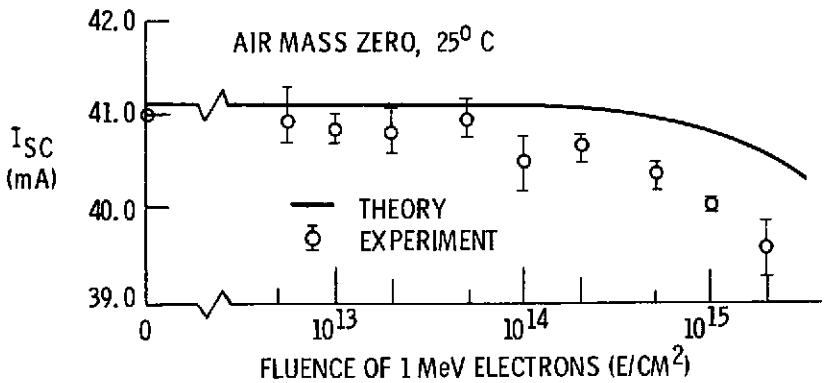

Fig. 9

E-7820

THEORETICAL EFFICIENCY OF THE EPITAXIAL BACK SURFACE FIELD CELL WITH SHORT SUBSTRATE DIFFUSION LENGTH

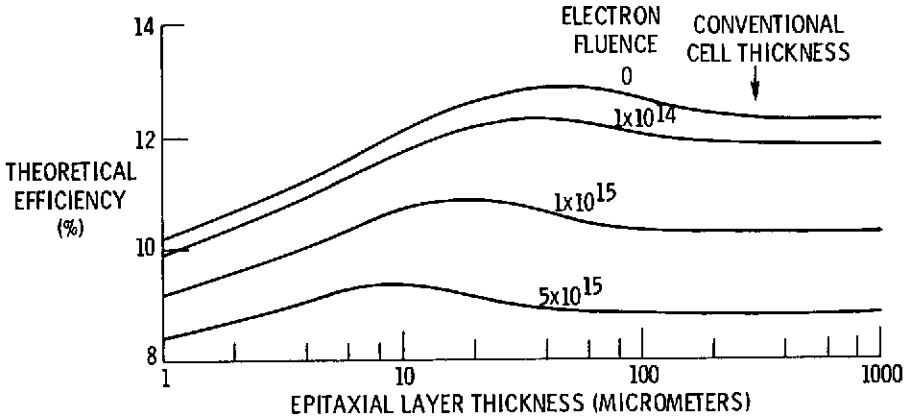

Fig. 10

THEORETICAL EFFICIENCY OF THE EPITAXIAL BACK SURFACE FIELD CELL WITH LONG SUBSTRATE DIFFUSION LENGTH

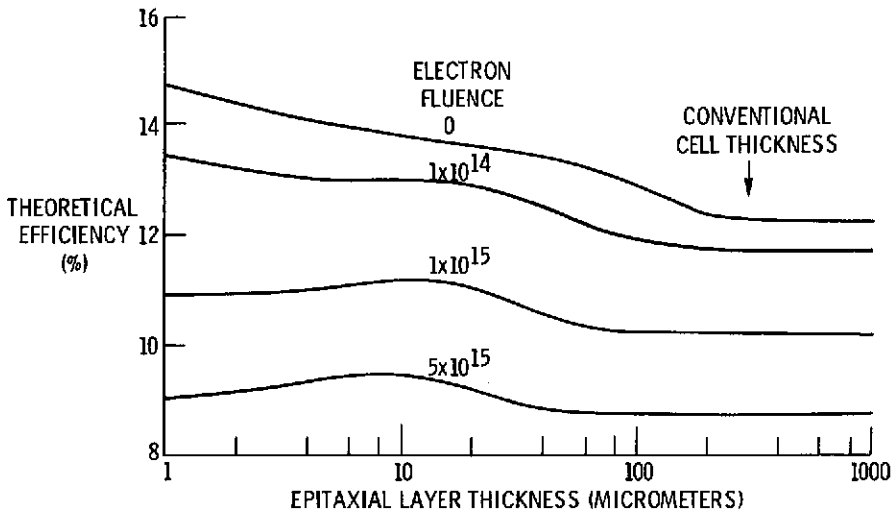

Fig. 11